

1 Article

2 Effect of silver decoration and light irradiation on the 3 antibacterial activity of TiO₂ and ZnO nanoparticles

4 Van Thang Nguyen¹, Tien Viet Vu¹, The Huu Nguyen¹,

5 Tuan Anh Nguyen², Thien Vuong Nguyen², Phuong Nguyen-Tri^{3,4*}

6 ¹ Faculty of Chemical Technology, Hanoi University of Industry, BacTu Liem, Hanoi, Vietnam; email:

7 thangnv2000@me.com

8 ²Institute for Tropical Technology, Vietnam Academy of Science and Technology, Hanoi, Vietnam; emails:

9 ntanh2007@gmail.com, vuongvast@gmail.com

10 ³Department of Chemistry, University of Montreal, Montreal, Quebec, Canada

11 Phuong.nguyen-tri@umontreal.ca

12 ⁴Département de chimie et physique, Université du Québec à Trois-Rivières, Québec, Canada

13 Phuong.Nguyen-Tri@uqtr.ca

14 * Correspondence: Phuong.nguyen-tri@umontreal.ca; Tel.: +514-340-5121 (ext. 7326)

15 Received: date; Accepted: date; Published: date

16 **Abstract:** This work emphasizes to use silver decorative method to enhance the antibacterial activity
17 of TiO₂ and ZnO nanoparticles. These silver decorated nanoparticles (hybrid nanoparticles) were
18 synthesized by using sodium borohydride as a reducing agent, with the weight ratio of Ag
19 precursors: oxide nanoparticles = 1: 30. The morphology and optical property of these hybrid
20 nanoparticles were investigated using transmission electron microscopy (TEM) and UV-vis
21 spectroscopy. The agar-well diffusion method was used to evaluate their antibacterial activity
22 against both *Staphylococcus aureus* and *Escherichia coli* bacteria, with or without light irradiation. The
23 TEM images indicated clearly that silver nanoparticles (AgNPs, 5-10 nm) were well deposited on
24 the surface of nano-TiO₂ particles (30-60 nm). Besides, smaller AgNPs (< 2 nm) were dispersed on
25 the surface of nano-ZnO particles (20-50 nm). UV-vis spectra confirmed that the hybridization of Ag
26 and oxide nanoparticles led to shift the absorption edge of oxide nanoparticles to the lower energy
27 region (visible region). The antibacterial tests indicated that both oxide pure nanoparticles did not
28 exhibit inhibitory against bacteria, with or without light irradiation. However, the presence of
29 AgNPs in their hybrids, even at low content (< 40 mg/mL) leads to a good antibacterial activity and
30 the higher inhibition zones under light irradiation as compared to that in dark was observed.

31 **Keywords:** Silver nanoparticles, nano-TiO₂, nano- ZnO, nanohybrids, antibacterial

32

33 1. Introduction

34 It was reported in literature that nanoparticles can attack bacteria through six main mechanisms
35 [1-15] such as: i) Destruction of the cell wall and peptidoglycan layer; ii) Release of toxic ions; iii)
36 Destruction of protons efflux bombs and modification of membrane charges; iv) Formation of reactive
37 oxygen species (ROS) degrading cell wall; v) Reactive oxygen species (ROS) degrading DNA, RNA
38 and proteins; vi) Low adenosintriphosphat (ATP) production. In case of metallic oxide nanoparticles
39 (such as NiO, Co₃O₄, ZnO, Fe₂O₃, Fe₃O₄, MgO, CuO, TiO₂, SiO₂...), ROS is the predominant
40 antibacterial mechanism, especially for nano-ZnO and Nano-TiO₂. For noble metal nanoparticles,
41 such as silver nanoparticles (AgNPs), they can attack effectively against both *Gram-negative* and
42 *Gram-positive* bacteria [16-19], via all 6 mentioned above antimicrobial mechanisms [20-22]. Therefore,
43 in the application AgNPs can be used as the sole antimicrobial agent. AgNPs could also react with
44 bacteria through the photo-catalytic production of ROS in solution [23]. However, Ag⁺ free ions
45 released from AgNPs are considered toxic not only to human cells, but also to the environment.
46 Loading (embedding/ immobilizing) AgNPs into oxide matrices is new approach due

47 to its ability to control solubility and toxicity of AgNPs. Various metallic oxide matrices have been
48 used for loading/hybridizing AgNPs, such SiO₂, ZrO₂, Al₂O₃, Fe₃O₄, CuO... [24].
49

50 Regarding the metal oxide semiconductor nanoparticles, such as ZnO and TiO₂, they can destroy
51 the pathogenic bacteria by ROS mechanism under UV light radiation. In this case, when a photon of
52 higher energy than their optical band gap energy (E_g~ 3.2-3.4 eV) is absorbed by these nanoparticles,
53 the electron-hole pairs were created and then generated ROS. The practical applications of these
54 nanoparticles are limited due to following two reasons: (i) wide band gap ~3.2 eV for nano-TiO₂
55 [25]; 3.37 eV for nano-ZnO [26]; and (ii) low photoenergy conversion efficiency [27] with low charge
56 separation efficiency and fast recombination of photogenerated charge carriers) [28, 29]. Two main
57 approaches have been tried to improve the photocatalytic of these nanoparticles: (1) diminution of the
58 recombination for photogenerated electron-hole pairs; and (2) enhancement of the visible light
59 sensitivity [25]. The first pathway focused on the design of heterostructures (heterojunctions), such
60 as (i) deposition of noble metals (Ag, Au or Pt) on the surface of nanoparticles; and (ii) coupling other
61 semiconductor (such as CdSe, Ag₂O, CdS...) with the oxide semiconducting nanoparticles [30-34]. The
62 formation of the Schottky barriers at the interface of noble metals/semiconducting oxide
63 nanoparticles could enhance significantly the segregation of charges, thus reduced the charge
64 recombination [35-36]. In this direction, under UV irradiation, Ubonchonlakate et al. [37] indicated
65 that Ag decorated TiO₂ had higher antibacterial activity (100 % in 10 min) against *P.aeruginosa*
66 bacteria, than that of pure TiO₂ (57% in 15 min). In other direction, the doping of transition metals/rare
67 earth ions into these oxide crystal lattices could reduce their optical band gap. For TiO₂, the
68 absorption edge was shifted into the lower energy region by S doping [38] and its absorption in visible
69 region increased with the doping content of noble metals [39].
70

71 Recently, the hybridization of noble metals (Au, Ag, Pd) and semiconducting oxides becomes
72 the most promising strategy to defeat large band gap of semiconducting oxides [40-44]. The energy
73 level alignment is combined at the heterojunction of these nanoparticles. In the hybrid nanoparticles,
74 the noble metal nanoparticles (gold and silver) exhibit Localized Surface Plasmon resonance (LSPR)
75 absorption in visible light region, which can have significant impact at the heterointerfaces. We
76 published several books and articles on the related topic [21, 40, 45, 64-79].
77

78 In this study, the hybridization of AgNPs and ZnO/TiO₂ nanoparticles are expected not only to
79 simply combine property of single components, but also to significantly enhance their antibacterial
80 properties [45]. Thus, this work aims to present the role of silver decoration in enhancing the
81 antibacterial activity of both ZnO and TiO₂ nanoparticles, against two most popular bacteria :
82 *Staphylococcus aureus* (ATCC 25923, Gram-positive) and *Escherichia coli* (Gram-negative, ATCC 25922).

83 2. Materials and Methods

84 2.1. Materials

85 TiO₂ (rutile) and ZnO nanoparticles, were purchased from Sigma Aldrich (Singapore), having a
86 mean diameter <100 nm and a specific surface area of 18 and 15-25 m²/g, respectively. AgNO₃ and
87 NaBH₄ were provided by Sigma Aldrich (Thailand).
88

89 2.2. Synthesis of silver decorated nanoparticles

90 0.2 g of TiO₂ (or ZnO) nanoparticles was firstly dispersed in 200 ml of distilled water under
91 ultrasonication. AgNO₃ solution (0.01 g in 20 ml water) then slowly added into the prepared nano-
92 TiO₂ (or ZnO) solution under ultrasonication in 30 m. The mixing solution then poured into the 500-
93 ml three-necked pot. Then, NaBH₄ solution (0.01 g in 30 ml water) was then added dropwise (1
94 drop/s) to the 500 ml three-necked pot. The reaction temperature was kept at 4 °C, and reaction
95 mixture was stirred mechanically for 60 minutes. The nanohybrids were then collected by using
96 centrifugation at 10 000 rpm/min for 5 minutes. The residual precursors and agents were then fully
97 removed after several times of centrifugation by adding fresh distilled water.

98

99 2.3. Characterization

100 The morphologies of the hybrid nanoparticles were investigated using transmission electron
101 microscopy (JEM1010, JEOL, Japan), operating at 80 kV (resolution of 3 Å). UV-Vis spectra were
102 obtained by using a CINTRA 40 spectrophotometer (USA) in absorbance mode with 2 nm slip width.

103

104 2.4. Antibacterial tests

105 The agar-well diffusion method was then used to evaluate their antibacterial activity against
106 Gram-positive (*Staphylococcus aureus* - ATCC 25923) and Gram-negative (*Escherichia coli* - ATCC
107 25922) bacteria. Nutrient agar plates were inoculated in brain heart infusion (BHI) broth using 100 µl
108 of 10⁶ CFU bacterial suspensions. Wells (8 mm diameter) were then punched in the inoculated plates,
109 by using a sterile plastic rod. These wells were then filled with 50 µL of solutions containing
110 nanoparticles, at various concentrations, such as 8, 16 and 40 mg/mL. Control wells were filled with
111 50 µL of distilled water. These plates were the incubated at 37 °C for 18 h (with or without light
112 irradiation). After this period, the antibacterial activities of these nanoparticles were evaluated by
113 measuring the inhibition zone diameter around the wells (100 µm resolution; Model: Haloes Caliper
114 - Zone Reader, IUL, Spain).

115

116 For light irradiation test, a LED (cold white, 1500 mcd, 3V DC) bulbs (two bulbs) has been used
117 with illumination of ~300 lux. These white LEDs were designed as mixture of blue (450-470 nm) and
118 yellow (560-590 nm) lights that could be perceived by the eye as white color [46].

119 3. Results and discussions**120 3.1. Morphological study**

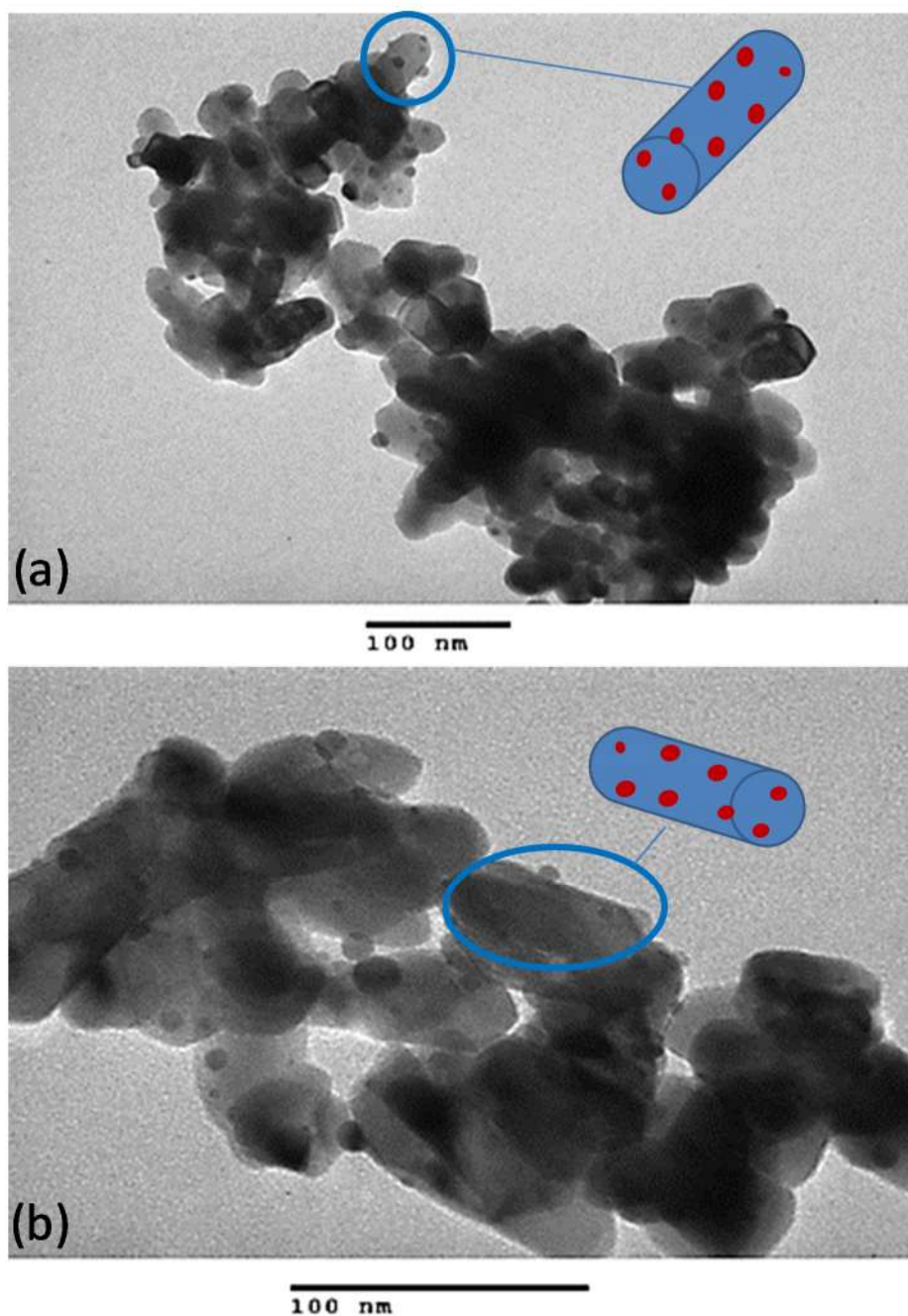
121 Figure 1 shows the electron microscopy images of AgNPs decorated nano-TiO₂ particles. As can
122 be seen in this figure, AgNPs (black particles, 5-10 nm) were well dispersed on the surface of nano-
123 TiO₂ particles (30-60 nm). The bigger nanoparticles are nano-TiO₂ and the smaller ones are AgNPs as
124 well described in the literature [21]. It has to be noted that the synthesis process of hybrid
125 nanoparticles was optimized to obtain the reported sizes of the hybrid nanoparticles.

126 TEM images of AgNPs decorated nano-ZnO particles are presented in Figure 2. As shown in this
127 figure, small AgNPs (black spots, < 2 nm) were alternatively deposited and linked to nano-ZnO
128 nanoparticles (10-30 nm). These small AgNPs might result in the presence of sharp peak at 410 nm in
129 the UV-vis spectra for these Ag/ZnO nanohybrids (Figure 4 below).

130 For a comparative study, the size of AgNPs deposited on surface of TiO₂ nanoparticles was higher
131 than that on surface of ZnO nanoparticles.

132

133



134

135

136

137

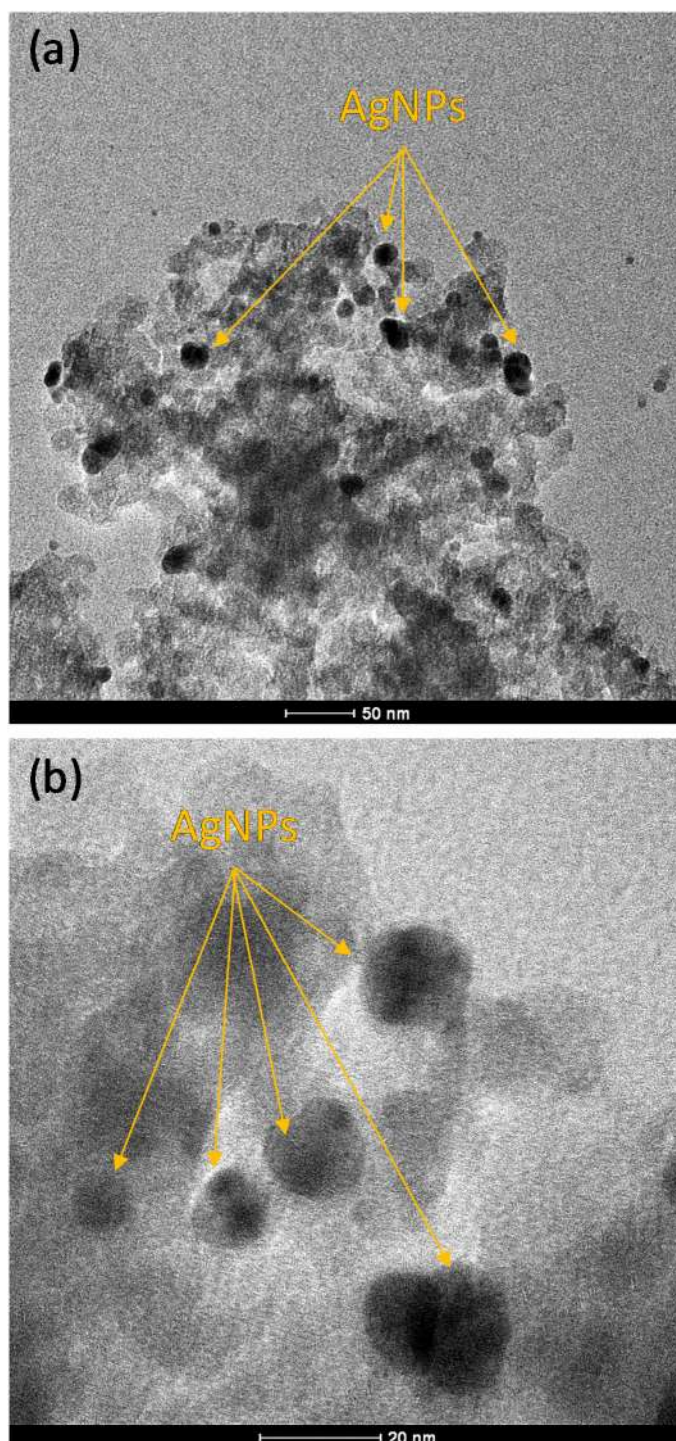
138

139

140

141

Figure 1. TEM images of Ag loaded TiO₂ nanoparticles at different magnifications showing the hybrid structure; a) 40,000x and b) 80,000x. Inserted images show the schematic illustration of hybrid nanoparticles. Red point represents Ag nanoparticles and blue support is nano-TiO₂

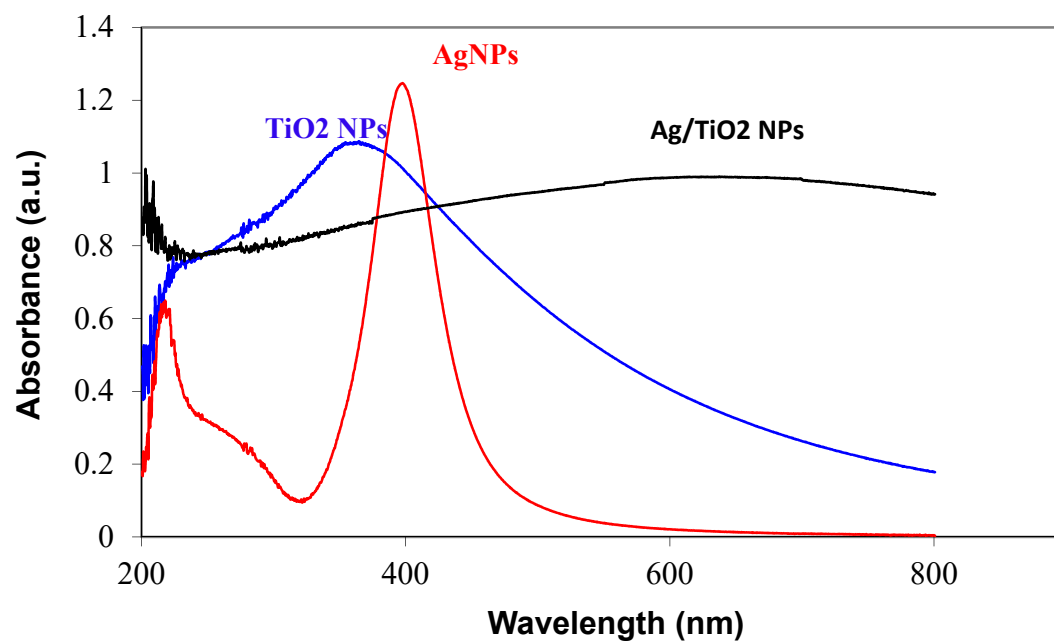


142
143 **Figure 2.** TEM images of Ag loaded ZnO nanoparticles at different magnification: a)
144 30,000x and b) 100,000x.
145

146 The UV-visible absorption spectra of AgNPs, nano-TiO₂ and AgNPs decorated nano-TiO₂
147 particles (dispersed in water) are presented in Figure 3. In case of AgNPs (~10 nm of diameter),
148 broad band around 398 nm was the characteristic of the Surface Plasmon Resonance (SPR peak) of
149 AgNPs [47]. For AgNPs decorated nano-TiO₂ particles, the hybridization of nano-TiO₂ and AgNPs
150 leads to shift the absorption edge to the lower energy region (visible region), as compared with the
151 pure nano-TiO₂ (at 360 nm in the UV region). Similar results were reported for Ag-TiO₂

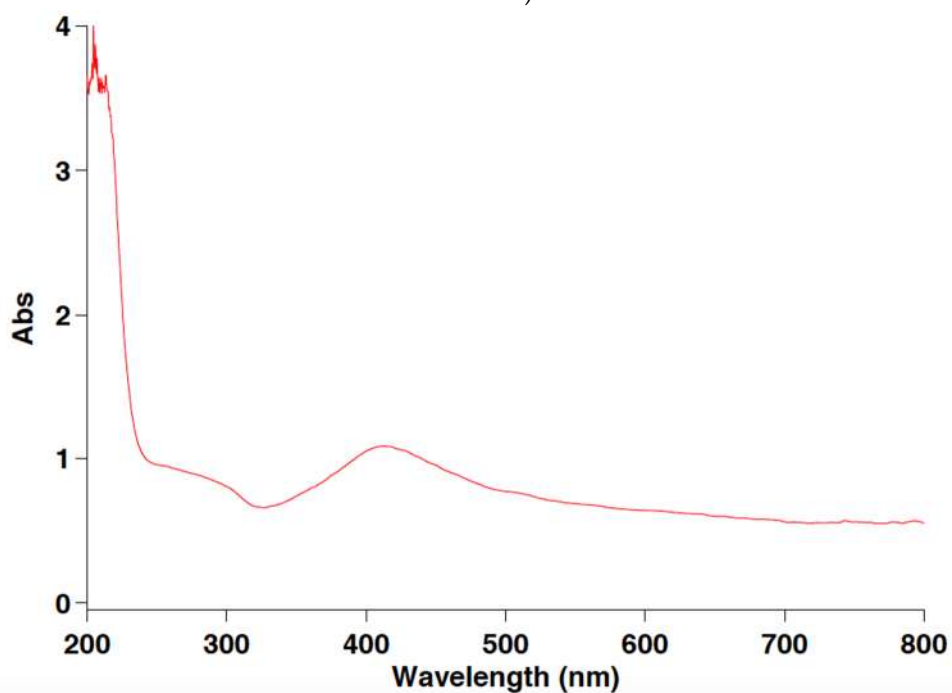
152 nanocomposites [48, 49]. The authors signaled that visible light absorption by Surface Plasmon
153 Resonance of AgNPs induced electron transfer to TiO₂, resulting in charge separation and therefore
154 activated by visible light.

155 Figure 4 shows the UV-visible spectra of AgNPs, nano-ZnO and AgNPs decorated nano-ZnO
156 particles (dispersed in water). As can be seen in Figure 4, a broad band around 410 nm was observed,
157 indicating the presence of AgNPs on the surface of nano-ZnO particles.



158

159 **Figure 3.** UV-Vis spectra of AgNPs, nano-TiO₂ and AgNPs decorated nano-TiO₂ particles (dispersed
160 in water)



161

162

163 **Figure 4.** UV-Vis spectra of AgNPs decorated nano-ZnO particles (dispersed in water)

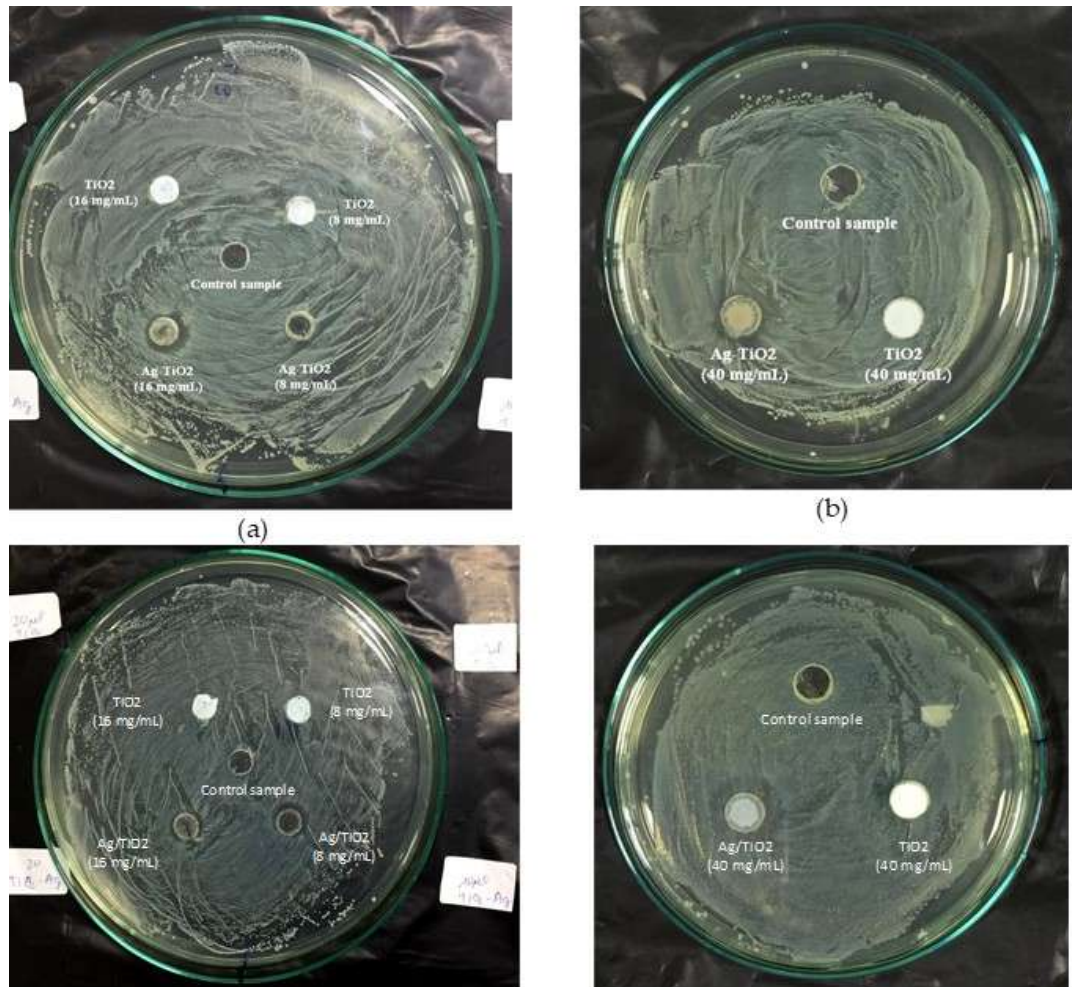
164 3.2. Antibacterial tests

165 3.2.1. TiO_2 and Ag/ TiO_2 nanoparticles

166 Figures 5 and 6 present the photographs of antibacterial test for nano- TiO_2 and Ag/ TiO_2 NPs
167 against *S. aureus* and *E. coli* bacteria, without and with light irradiation, respectively. Tables 1 and 2
168 show their corresponding inhibition zones. As shown in Figures 5a and 5b, in the dark TiO_2 NPs did
169 not exhibit inhibitory effects on *S. aureus* bacteria (at concentrations of 10-40 mg/mL), whereas Ag
170 loaded TiO_2 NPs exhibited significant antibacterial activity at the concentration of 40 mg/mL). It was
171 reported that TiO_2 nanoparticles are easy to attach to the cell membranes and accumulate [50]. In
172 general, TiO_2 nanoparticles can destroy the pathogenic bacteria by ROS mechanism under UV light
173 radiation. Since the emitted wavelengths of the white LED lights include peaks in the blue (450-470
174 nm) and yellow (560-590nm) areas, the inhibition zone of Ag loaded TiO_2 NPs (40 mg/mL) could be
175 attributed to the content of AgNPs in the nanohybrids (e.g ~1.3 mg/mL). Please note that the
176 concentration of TiO_2 in nanohybrids is 30 times higher than that of AgNPs (from synthesis: the
177 weight ratio of Ag precursors: TiO_2 = 1: 30). Besides, Ubonchonlakate et al. [51] reported that Ag
178 doped TiO_2 had higher antibacterial efficiency (100 % in 10 min) against *P. Aeruginosa* bacteria than
179 that of pure TiO_2 (57% in 15 min), under UV irradiation. The interesting results are observed under
180 light irradiation for Ag/ TiO_2 nanohybrids (Table 1). These nanoparticles exhibited the inhibition zone
181 of 2 mm (in diameter) at the lower concentration of 16 mg/mL, indicating the contribution of TiO_2
182 nanoparticles in this nanohybrids to their antibacterial activity. At the high concentration of 40
183 mg/mL, their inhibition zone is similar to the case in dark (4 mm in diameter), indicating the
184 dominated contribution of AgNPs to the antibacterial activity of these nanohybrids (at this high
185 concentration).

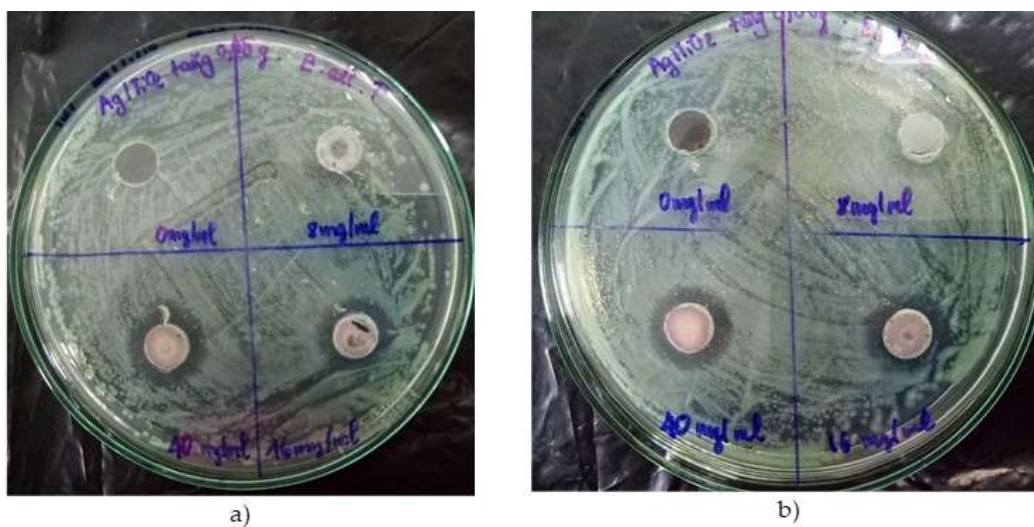
186
187 As seen in Figures 5c and 5d, TiO_2 NPs did not exhibit inhibitory effects under this light
188 irradiation on these bacteria (at concentration of 8-40 mg/mL). It was reported that the absorption of
189 light in the visible region of TiO_2 increased with the noble metals (Pt, Au and Pd) doping content [52].
190 Yue Lin et al. [53] also reported the antibacterial properties against *E.coli* of the Ag/ TiO_2 core/shell
191 nanoparticles without the presence of UV light. They observed the obvious zone of inhibition around
192 the hybrid nanoparticles, whereas there was no inhibition detected around the pure TiO_2
193 nanoparticles. Similar results also were observed by Dhanalekshmi et al [54] for Ag/ TiO_2 core/shell
194 hybrid nanoparticles against *E.coli* and *S.aureus* bacteria. Zhang et al. [55] reported TiO_2 nanoparticles
195 with highly dispersed Ag clusters are entirely restricted the *E. coli* bacterial growth [55]. Barudin et
196 al. [56] indicated that Ag- TiO_2 nanoparticles exhibited the superior antibacterial activity, as compared
197 to the lone individual TiO_2 nanoparticles, under visible light irradiation [56].

198 In this work, for *E.coli* bacteria, under light irradiation Ag/ TiO_2 nanohybrids have the higher
199 antibacterial activity than that in darkness (Table 2, with concentration of 8 and 16 mg/mL), due to
200 the hybridization of AgNPs and TiO_2 NPs. Besides, in dark, the inhibition zones of Ag/ TiO_2
201 nanohybrids increase with their concentration, due to the increase of AgNPs in the nanohybrids.



202
203
204
205

Figure 5. Photographs of antibacterial test against *S. aureus* bacteria (agar-well diffusion method) for pure TiO₂ and Ag loaded TiO₂ nanoparticles (a and b: without light irradiation; c and d: without light irradiation). Concentrations of 8, 16 and 40 mg/mL.



206

207 **Figure 6.** Photographs of antibacterial test against *E. coli* bacteria (agar-well diffusion
208 method) for Ag loaded TiO₂ nanoparticles: a) without light irradiation; b) under light irradiation).
209 Concentration of 8, 16 and 40 mg/mL.

210

211 Table 1: Antibacterial activity against *S. aureus* bacteria of TiO₂ nanoparticles and Ag loaded
212 TiO₂ nanoparticles

Concentrations (mg/mL)	Inhibition Zone (mm)			
	without light irradiation		under light irradiation	
	TiO ₂ nanoparticles	Ag decorated TiO ₂ nanoparticles	TiO ₂ nanoparticles	Ag decorated TiO ₂ nanoparticles
8	0	0	0	0
16	0	0	0	2
40	0	4	0	4

213

214

215 Table 2: Antibacterial activity against *E. coli* bacteria of TiO₂ nanoparticles and Ag loaded
216 TiO₂ nanoparticles

Concentrations (mg/mL)	Inhibition Zone (mm)			
	without light irradiation		under light irradiation	
	TiO ₂ nanoparticles	Ag decorated TiO ₂ nanoparticles	TiO ₂ nanoparticles	Ag decorated TiO ₂ nanoparticles
8	0	2	0	6
16	0	6	0	8
40	0	8	0	8

217

218

219 3.2.2. ZnO and Ag/ZnO nanoparticles

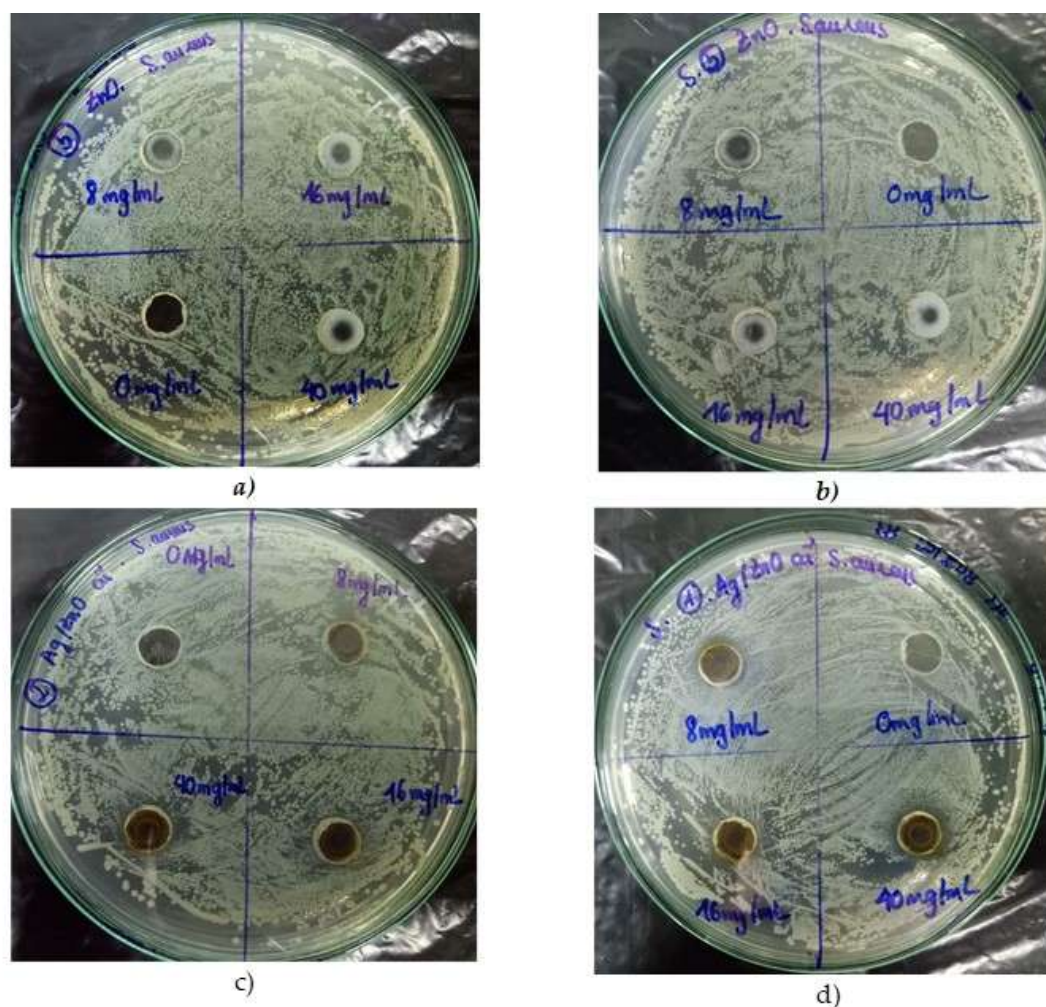
220 It was reported in literature that ZnO has the inherent gain of broad antibacterial activities
221 against virus, bacteria, fungus and spores [57-59]. Stoimenov et al. [60] defined that ZnO
222 nanoparticles attached on the bacterial surface due to electrostatic force of attraction. We expect that
223 the hybridization of AgNPs with ZnO NPs may exhibit the superior antibacterial activity, as
224 compared to the lone individual NPs [45].

225 Figures 7 and 8 show the photographs of antibacterial test for nano-ZnO and Ag/ZnO NPs
226 against *S. aureus* and *E. coli* bacteria, without and with light irradiation, respectively. Tables 3 and 4
227 show their corresponding inhibition zones. As shown in Figures 7 and 8, ZnO NPs did not exhibit
228 inhibitory effects on both bacteria with or without light irradiation (at concentrations of 10-40
229 mg/mL).

230 For Ag/ZnO nanohybrids, as shown in Tables 3 and 4, light irradiation increases the diameter
231 of inhibition zone for both *S. aureus* (at 8 mg/mL) and *E. coli* (at 8, 16, 40 mg/mL) bacteria. Similarity,
232 Mariana Ibanescu et al. [61] reported the antimicrobial property of Ag/ZnO nanocomposites against
233 both *E. coli* and *M. luteus* bacteria. The authors found that small amounts of silver could significantly
234 enhance the antimicrobial activity. The photocatalytic activity of Ag/ZnO nanocomposites could
235 contribute to their high antimicrobial activity. Nagaraju et al. [62] also indicated the high

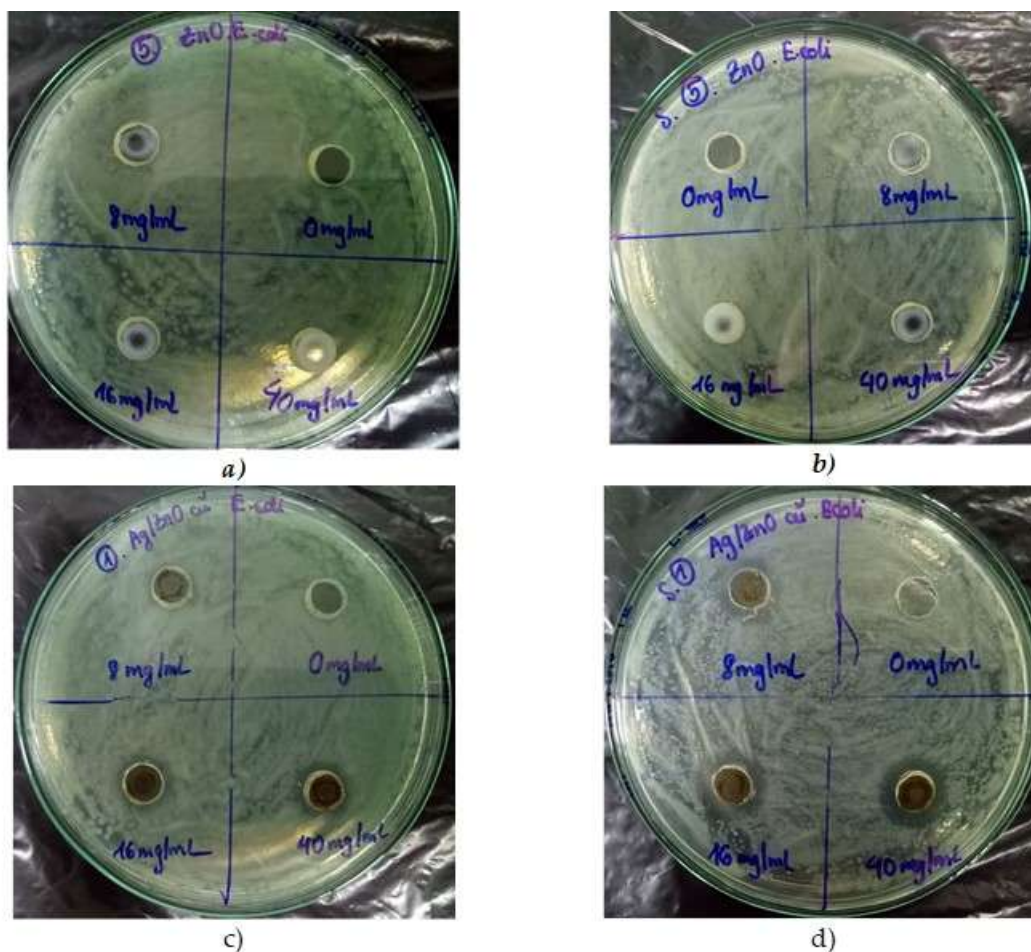
236 antimicrobial activity of Ag-ZnO NPs against both *E. coli* and *S. aureus* bacteria. The inhibition zone
237 could be observed at the concentration of 500 μg Ag-ZnO NPs. Wei et al. [63] also described the high
238 antibacterial activity of Ag-ZnO hybrid nanofibres against *E. coli* and *P. aeruginosa* bacteria.

239 For the comparative study, under light irradiation at the low concentration (8 mg/mL), Ag/ZnO
240 nano hybrids exhibit the higher antibacterial activity against both two bacteria, than Ag-Ag/TiO₂
241 nano hybrids. One possible explanation is the better homogeneous deposition of the smaller AgNPs
242 on the surface of nano-ZnO particles, as compared to that of nano-TiO₂ nanoparticles (Figures 1 and
243 2).
244



245 **Figure 7.** Photographs of antibacterial test against *S. aureus* bacteria (agar-well diffusion
246 method) for pure ZnO nanoparticles (a: without light irradiation; b: under light irradiation) and Ag
247 loaded ZnO nanoparticles (c: without light irradiation; d: under light irradiation). Concentration of
248 8, 16 and 40 mg/mL.

249
250



251

252

253

254

255

256

257

258

259

Figure 8. Photographs of antibacterial test against *E. coli* bacteria (agar-well diffusion method) for ZnO nanoparticles (a-without light irradiation; b-under light irradiation) and Ag loaded ZnO nanoparticles (c-without light irradiation; d-under light irradiation). Concentration of 8, 16 and 40 mg/mL.

Table 3: Antibacterial activity against *S. aureus* bacteria of ZnO nanoparticles and Ag loaded ZnO nanoparticles

Concentrations (mg/mL)	Inhibition Zone (mm)					
	without light irradiation			under light irradiation		
	ZnO nanoparticles	Ag decorated ZnO nanoparticles		ZnO nanoparticles	Ag decorated ZnO nanoparticles	
8	0	0		0	2	
16	0	2		0	2	
40	0	4		0	4	

260

261

262

263
264
265Table 4: Antibacterial activity against *E. coli* bacteria of ZnO nanoparticles and Ag loaded

Concentrations (mg/mL)	ZnO nanoparticles					
	without light irradiation			under light irradiation		
	ZnO nanoparticles	Ag decorated ZnO nanoparticles		ZnO nanoparticles	Ag decorated ZnO nanoparticles	
8	0	2	0	7		
16	0	4	0	8		
40	0	6	0	8		

266

267 **4. Conclusions**

268 The main findings of this work were as follows:

- 269 1. Silver decorated oxide nanoparticles have been successfully synthesized by using
270 sodium borohydride as reducing agent, with the weight ratio of Ag precursors: oxide
271 nanoparticles = 1: 30.
- 272 2. The TEM images indicated that AgNPs (5-10 nm) were deposited on the surface of nano-
273 TiO₂ particles (30-60 nm). Whereas, the smaller AgNPs (< 2 nm) were dispersed on the
274 surface of nano-ZnO particles (10-30 nm).
- 275 3. UV-vis spectra indicated that the hybridization of Ag and oxide nanoparticles led to
276 shift the absorption edge of oxide nanoparticles to the lower energy region (visible
277 region).
- 278 4. The antibacterial tests indicated that both oxide nanoparticles did not exhibit inhibitory
279 against bacteria, with or without light irradiation. However, the presence of AgNPs in
280 their hybrids (at the concentration < 40 mg/mL) exhibited the higher inhibition zones
281 under light irradiation, as compared to that in dark. At the high concentration of 40
282 mg/mL, the antibacterial behavior of these nanohybrids under light irradiation is similar
283 to that in dark, indicating the dominated contribution of AgNPs to the antibacterial
284 activity of these nanohybrids (at this high concentration).
- 285 5. As the comparative study, under light irradiation at the low concentration (8 mg/mL),
286 Ag/ZnO nanohybrids exhibit the higher antibacterial activity against both two bacteria,
287 than the Ag-Ag/TiO₂ nanohybrids.

288 **Author Contributions:** Conceptualization and methodology, N.T.P.; N.T.A; synthesis of ZnO-AgNPs: T.V.V and
289 N.T.V; Synthesis of TiO₂-AgNPs: T.H.N; writing—original draft preparation, N.T.A; writing—review and
290 editing N.T.P.; supervision, N.T.P.;

291 **Funding:** This work was financial supported by Natural Sciences and Engineering Research Council of Canada
292 (NSERC).

293 **Conflicts of Interest:** The authors declare no conflict of interest.

294 **References**

- 295 1. Rai VR, Bai AJ., Nanoparticles and their potential application as antimicrobials. In: Science against
296 microbial pathogens: Communicating current research and technological advances, Méndez-Vilas A. Ed.,
297 Formatex, Microbiology Series No.3, Vol.1, Badajoz, Spain. 97-209, 2011.
- 298 2. BECON Nanoscience and Nanotechnology Symposium Report, National Institutes of Health
299 Bioengineering Consortium, National Institute of Health, USA, 2000. <http://www.uta.edu/rfmems/060515-NSF-NUE/Info/biomed/nanotechsympreport.pdf>
300

- 301 3. Q. Li, S Mahendra, D Y Lyon, L Brunet, MV Liga, D Li, P J J Alvarez, Antimicrobial nanomaterials for water
302 disinfection and microbial control: Potential applications and implications. *Water Res.*, 42 (2008) 4591–4602
303 4. E. Oesterling, N Chopra, V Gavalas, X Arzuaga, E J Lim, R Sultanab, D A Butterfield, L Bachas, B Hennig,
304 Alumina nanoparticles induce expression of endothelial cell adhesion molecules. *Toxicol Lett.*, 178 (2008)
305 160-166.
306 5. S. Dey, V. Bakthavatchalu, M. T . Tseng, P. Wu, R. L. Florence, E. A. Grulke, R. A. Yokel, S. K. Dhar, H. S.
307 Yang, Y. Chen, D. K. St Clair, Interactions between SIRT1 and AP-1 reveal a mechanistic insight into the
308 growth promoting properties of alumina (Al₂O₃) nanoparticles in mouse skin epithelial cells,
309 *Carcinogenesis*, 29 (2008) 1920–1929.
310 6. Y. N. Chang, M Zhang, L Xia, J Zhang, G Xing, The Toxic Effects and Mechanisms of CuO and ZnO
311 Nanoparticles, *Materials*, 5 (2012) 2850-2871.
312 7. H. L. Karlsson, P Cronholm, J Gustafsson, L Moller, Copper oxide nanoparticles are highly toxic: A
313 comparison between metal oxide nanoparticles and carbon nanotubes, *Chem Res Toxicol.* 21 (2008)1726–
314 1732.
315 8. T. Xia, M. Kovoichich, M. Liong, L. Mädler, B. Gilbert, H. Shi, J. I. Yeh, J. I. Zink, A. E. Nel, Comparison of
316 the mechanism of toxicity of zinc oxide and cerium oxide nanoparticles based on dissolution and oxidative
317 stress properties, *ACS Nano.* 23 (2008) 2121-2134.
318 9. S. M. Hussain, K. L. Hess, J. M. Gearhart, K. T. Geiss, J. J. Schlager, In vitro toxicity of nanoparticles in BRL
319 3A rat liver cells, *Toxicol In Vitro.* 19 (2005) 975–983.
320 10. G Ren, D Hu, EW Cheng, MA Vargas-Reus, P Reip, RP Allaker, Characterisation of copper oxide
321 nanoparticles for antimicrobial applications. *J Antimicrob Agents.*, 33(2009) 587-90.
322 11. J Niskanen, J Shan, H Tenhu, H Jiang, E Kauppinen, V Barranco, F Pico, K Yliniemi, K. Kontturi, Synthesis
323 of copolymerstabilized silver nanoparticles for coating materials. *Colloid Polym Sci.* 288 (2010) 543–553.
324 12. J P Guggenbichler, M Böswald, S Lugauer, T Krall, A new technology of microdispersed silver in
325 polyurethane induces antimicrobial activity in central venous catheters, *Infection*, 27 Suppl 1 (1999) S16-23.
326 13. A Azam, AS Ahmed, M Oves, MS Khan, A. Memic, Size-dependent antimicrobial properties of CuO
327 nanoparticles against Gram-positive and -negative bacterial strains *Int J Nanomedicine*, 7 (2012) 3527–3535.
328 14. RP. Allaker, The use of nanoparticles to control oral biofilm formation, *J dent Res.* 89 (2010) 1175-1185.
329 15. C. L. Santos, A. J. R. Albuquerque, F. C. Sampaio and D. Keyson, Nanomaterials with Antimicrobial
330 Properties: Applications in Health Sciences, In: *Microbial pathogens and strategies for combating them:*
331 *Science, Technology and Education*, A. Méndez-Vilas Ed., Formatex, 2013, Badajoz, Spain.
332 16. H. H. Huang, X. P. Ni, G. L. Loy, C. H. Chew, K. L. Tan, F. C. Loh, J. F. Deng, and G. Q. Xu, Photochemical
333 Formation of Silver Nanoparticles in Poly(N-vinylpyrrolidone), *Langmuir* 12 (1996) 909-912. DOI:
334 10.1021/la950435d
335 17. E. Weir, A. Lawlor, A. Whelan, and F. Regan, The use of nanoparticles in anti-microbial materials and their
336 characterization, *Analyst* 133 (2008) 835-845. doi: 10.1039/b715532h.
337 18. C M Jones, E M V Hoek, A review of the antibacterial effects of silver nanomaterials and potential
338 implications for human health and the environment, *J. Nanopart. Res.* 12 (5) (2010) 1531-1551.
339 19. M.A. Shenashen, S.A. El-Safty, E.A. Elshehy, Synthesis, morphological control, and properties of
340 silver nanoparticles in potential applications, *Part. Part. Syst. Charact.* 31 (2014) 293–316,
341 doi:10.1002/ppsc.201300181.
342 20. Q Li, S Mahendra, DY Lyon, L Brunet, MV Liga, D Li, P J J Alvarez, Antimicrobial nanomaterials for
343 water disinfection and microbial control: Potential applications and implications, *Water Res.* 42 (2008)
344 4591–4602
345 21. P. Nguyen-Tri, V. T. Nguyen, T. A. Nguyen, Biological activity and nanostructuring of Fe₃O₄-Ag
346 /polyethylene nanocomposites, *Journal of Composites Science*, 2019, 3 (2)
347 <https://doi.org/10.3390/jcs474493>
348 22. SM Hussain, KL Hess, JM Gearhart, KT Geiss, JJ Schlager, In vitro toxicity of nanoparticles in BRL 3A rat
349 liver cells, *Toxicol In Vitro.* 19(2005) 975–983.
350 23. B. Le Ouay, F. Stellacci, Antibacterial activity of silver nanoparticles: a surface science insight, *Nano Today*
351 10 (2015) 339–354, doi:10.1016/j.nantod.2015.04.002.
352 24. K. I. Dhanalekshmi, Van Thang Nguyen, P. Magesan, Chapter 26: Nanosilver loaded oxide nanoparticles
353 for antibacterial application, In: “*Smart nanocontainers: Fundamentals and Emerging Applications*”, Eds:
354 Phuong Nguyen-Tri, Trong-On Do, Tuan Anh Nguyen, (2019) Elsevier. ISBN: 9780128167700

- 355 25. O. Akhavan, Lasting antibacterial activities of Ag-TiO₂/Ag/a-TiO₂ nanocomposite thin film photocatalysts
356 under solar light irradiation, *Journal of Colloid and Interface Science*, 336 (1) 2009 117-124.
357 <https://doi.org/10.1016/j.jcis.2009.03.018>
- 358 26. H. Gholap, S. Warule, J. Sangshetti, G. Kulkarni, A. Banpurkar, S. Satpute, R. Patil, Hierarchical
359 nanostructures of Au@ZnO: antibacterial and antibiofilm agent, *Appl Microbiol Biotechnol*, 100 (13) (2016)
360 5849-5858. doi: 10.1007/s00253-016-7391-1
- 361 27. Y Tamaki, K Hara, R Katoh, M Tachiya, A Furub Femtosecond visible-to-IR spectroscopy of TiO₂
362 nanocrystalline films: elucidation of the electron mobility before deep trapping. *J Phys Chem C*, 113 (2009)
363 11741-11746
- 364 28. X. Chen, S.S. Mao, Titanium dioxide nanomaterials: synthesis, properties, modifications and applications,
365 *Chem. Rev.* 107 (2007) 2891-2959.
- 366 29. A. Kudo, Y. Miseki, Heterogeneous photocatalyst materials for water splitting, *Chem. Soc. Rev.* 38 (2009)
367 253-278
- 368 30. L. Sun, J. Li, C. Wang, S. Li, Y. Lai, H. Chen, C. Lin, Ultrasound aided photochemical synthesis of Ag loaded
369 TiO₂ nanotube arrays to enhance photocatalytic activity, *J. Hazard. Mater.* 171 (2009) 1045-1050.
- 370 31. Md. A. A. Mamun, Y. Kusumoto, T. Zannat, S. Md Islam, Synergistic enhanced photocatalytic and
371 photothermal activity of Au@TiO₂ nanopellets against human epithelial carcinoma cells, *Phys. Chem.*
372 *Chem. Phys.* 13 (2011) 21026-21034.
- 373 32. J.S. Jang, S.H. Choi, H.G. Kim, J.S. Lee, Location and state of Pt in platinumized CdS/TiO₂ photocatalysts for
374 hydrogen production from water under visible light, *J. Phys. Chem. C* 112 (2008) 17200-17205.
- 375 33. D. Sarkar, C.K. Ghosh, S. Mukherjee, K.K. Chattopadhyay, Three dimensional Ag₂O/TiO₂ type-II (p-n)
376 nanoheterojunctions for superior photocatalytic activity, *ACS Appl. Mater. Interfaces* 5 (2013) 331-337.
- 377 34. Y.F. Ji, W. Guo, H.H. Chen, L.S. Zhang, S. Chen, M.T. Hua, Y.H. Long, Z. Chen Surface Ti³⁺/Ti⁴⁺ redox
378 shuttle enhancing photocatalytic H₂ production in ultrathin TiO₂ nanosheets/CdSe quantum dots, *J. Phys.*
379 *Chem. C* 119 (2015) 27053-7059.
- 380 35. Q. Deng, H.B. Tang, G. Liu, X.P. Song, G.P. Xu, Q. Li, D.H.L. Ng, G.Z. Wang, The fabrication and
381 photocatalytic performances of flower-like Ag nanoparticles/ZnO nanosheets-assembled microspheres,
382 *Appl. Surf. Sci.* 331(2015) 50-57.
- 383 36. Y.M. Liang, N. Guo, L.L. Li, R.Q. Li, G.J. Ji, S.C. Gan, Fabrication of porous 3D flower-like Ag/ZnO
384 heterostructure composites with enhanced photocatalytic performance, *Appl. Surf. Sci.* 332 (2015) 32-39.
- 385 37. K. Ubonchonlakate, L. Sikong, F. Saito, Photocatalytic disinfection of *P.aeruginosa* bacterial Ag-doped TiO₂
386 film, *Procedia Eng.* 32 (2012) 656-662.
- 387 38. T. Umebayashi, T. Yamaki, S. Tanaka, K. Asai, Visible light-induced degradation of methylene blue on S-
388 doped TiO₂, *Chem. Lett.* 32 (2003) 330-331.
- 389 39. S. Sakthivel, M.V. Shankar, M. Palanichamy, B. Arabindoo, D.W. Bahnemann, V. Murugesan, Enhancement
390 of photocatalytic activity by metal deposition: characterisation and photonic efficiency of Pt, Au and Pd
391 deposited on TiO₂ catalyst, *Water Res.* 38 (2004) 3001-3008.
- 392 40. Mohapatra, S.; Nguyen, T.A.; Nguyen-Tri, P. *Noble Metal-Metal Oxide Hybrid Nanoparticles: Fundamentals and Applications*; Elsevier: Amsterdam, The Netherlands, 2018; Volume 1.
- 393 41. Fageria, P., Gangopadhyay, S. & Pande, S. Synthesis of ZnO/Au and ZnO/Ag nanoparticles and their
394 photocatalytic application using UV and visible light. *RSC Adv.* 4, 24962-24972, doi:10.1039/c4ra03158j
395 (2014).
- 396 42. Xu, C. et al. Fabrication of visible-light-driven Ag/TiO₂ heterojunction composites induced by shock wave.
397 *Journal of Alloys and Compounds* 679, 463-469, doi:10.1016/j.jallcom.2016.04.048 (2016).
- 398 43. Xu, F. et al. Au nanoparticles modified branched TiO₂ nanorod array arranged with ultrathin nanorods for
399 enhanced photoelectrochemical water splitting. *Journal of Alloys and Compounds* 693, 1124-1132,
400 doi:10.1016/j.jallcom.2016.09.273 (2017).
- 401 44. Chang, Y. et al. Optical Properties and Photocatalytic Performances of Pd Modified ZnO Samples. *The*
402 *Journal of Physical Chemistry C* 113, 18761-18767, doi:10.1021/jp9050808 (2009).
- 403 45. Phuong Nguyen Tri, Tuan Anh Nguyen, The Huu Nguyen, Pascal Carriere, Antibacterial Behavior of
404 Hybrid Nanoparticles (Chapter 7), In: "Noble Metal-Metal Oxide Hybrid Nanoparticles: Fundamentals and
405 Applications", Eds: Satyabrata Mohapatra, Tuan Anh Nguyen, Phuong Nguyen-Tri (2019) 141-155.
406 Elsevier, <https://doi.org/10.1016/B978-0-12-814134-2.00007-3>
407

- 408 46. Standard and White LED Basics and Operation, <https://www.maximintegrated.com/en/app->
409 [notes/index.mvp/id/3070](https://www.maximintegrated.com/en/app-)
- 410 47. Kuriakose, S., Choudhary, V., Satpati, B. & Mohapatra, S. Enhanced photocatalytic activity of Ag-ZnO
411 hybrid plasmonic nanostructures prepared by a facile wet chemical method. *Beilstein J Nanotechnol* 5, 639-
412 650, doi:10.3762/bjnano.5.75 (2014).
- 413 48. M. K. Seery, R. George, P. Floris, S.C. Pillai, Silver doped titanium dioxide nanomaterials for enhanced
414 visible light photocatalysis, *J. Photochem. Photobiol. A*, 189 (2-3) (2007) 258-263.
415 <https://doi.org/10.1016/j.jphotochem.2007.02.010>
- 416 49. Y. Tian, T. Tatsuma, Plasmon-induced photoelectrochemistry at metal nanoparticles supported on
417 nanoporous TiO₂, *Chem. Commun.* 16 (2004) 1810-1811. DOI: 10.1039/B405061D
- 418 50. R. Cai, K. Hashimoto, K. Itoh, Y. Kubota, A. Fujishima, Photokilling of Malignant cells with ultrafine TiO₂
419 powders, *Bull.Chem. Soc.* 64 (1991) 1268-1273
- 420 51. K. Ubonchonlakate, L. Sikong, F. Saito, Photocatalytic disinfection of P.aeruginosa bacterial Ag-doped TiO₂
421 film, *Procedia Eng.* 32 (2012) 656-662.
- 422 52. S. Sakthivel, M.V. Shankar, M. Palanichamy, B. Arabindoo, D.W. Bahnemann, V. Murugesan, Enhancement
423 of photocatalytic activity by metal deposition: characterisation and photonic efficiency of Pt, Au and Pd
424 deposited on TiO₂ catalyst, *Water Res.* 38 (2004) 3001-3008
- 425 53. L. Yue, Q. Wang, X. Zhang, Z. Wang, W. Xia, Y. Dong, Synthesis of Ag/TiO₂ Core/Shell Nanoparticles with
426 Antibacterial Properties, *Bull. Korean Chem. Soc.*, 32 (8) (2011) 2607-2610. DOI :
427 10.5012/bkcs.2011.32.8.2607
- 428 54. K. I. Dhanalekshmi, K. S. Meen, I. Ramesh, Synthesis and Characterization of Ag@TiO₂ Core-shell
429 nanoparticles and study of its antibacterial activity, *International Journal of Nanotechnology and*
430 *Application*, 3 (5) (2013) 5-14
- 431 55. H. Zhang, G. Chen, Potent Antibacterial Activities of Ag/TiO₂ Nanocomposite Powders Synthesized by a
432 One-Pot Sol-Gel Method, *Environ. Sci. Technol.* 43 (8) (2009) 2905-2910
- 433 56. Nur Hidayati Ahmad Barudin, Srimala Sreekantan, Ong Ming Thong, Geetha Sahgal, Antibacterial
434 Activity of Ag-TiO₂ Nanoparticles with Various Silver Contents *Materials Science Forum* Vol. 756 (2013)
435 238-245.
- 436 57. T Jin, D Sun, JY Su, H Zhang, HJ Sue, Antimicrobial Efficacy of Zinc Oxide Quantum Dots against *Listeria*
437 *monocytogenes*, *Salmonella Enteritidis*, and *Escherichia coli* O157:H7. *74(1)* (2009) M46-M52
- 438 58. K. M. Kumar, B. K. Mandal, E. A. Naidu, M. Sinha, K. S. Kumar, P. S. Reddy, Synthesis and Characterization
439 of Flower Shaped Zinc Oxide Nanostructures and Its Antimicrobial Activity. *Spectrochim. Acta, Part A*,
440 104 (2013) 171-174.
- 441 59. A. Lipovsky, Y. Nitzan, A. Gedanken, R. Lubart, Antifungal Activity of ZnO Nanoparticles - the Role of
442 ROS Mediated Cell Injury. *Nanotechnology*, 22 (2011) 105101.
- 443 60. P K Stoimenov, R L Klinger, G L Marchin, K J Klabunde, Metal oxide nanoparticles as bactericidal agents.
444 *Langmuir* 18 (2002) 6679-6686
- 445 61. Mariana Ibanescu, Viorica Mușat, Torsten Textor, Viorel Badilita Boris Mahltig, Photocatalytic and
446 antimicrobial Ag/ZnO nanocomposites for functionalization of textile fabrics, *Journal of Alloys and*
447 *Compounds*, 610 (2014) 244-249.
- 448 62. G. Nagaraju, Udayabhanu, Shivaraj, S.A. Prashanth, M. Shastri, K.V. Yathish, C. Anupama, D. Rangappa,
449 Electrochemical heavy metal detection, photocatalytic, photoluminescence, biodiesel production and
450 antibacterial activities of Ag-ZnO nanomaterial, *Materials Research Bulletin*, 94 (2017) 54-63.
- 451 63. Y. Wei, Y. B. Chong, H. Du, J. Kong, C. He, Loose Yarn of Ag-ZnO-PAN/ITO Hybrid Nanofibres:
452 Preparation, Characterization and Antibacterial Evaluation, *Materials & Design*, 139 (2018) 153-161.
- 453 64. Phuong, N.-T., Rtimi S., Claudiane Ouellet Plamondon. *Nanomaterials Based Coatings: Fundamentals and*
454 *Applications*; Elsevier: Amsterdam, The Netherlands, 2019. ISBN: 9780128158845.
- 455 65. Nguyen Tri, P.; Guinault, A.; Sollogoub, C. Élaboration et propriétés des composites polypropylène
456 recyclé/fibres de bambou. *Matér. Tech.* 2012, 100, 413-423. [Google Scholar] [CrossRef][Green Version]
- 457 66. Azizi, S.; David, E.; Fréchet, M.F.; Nguyen-Tri, P.; Ouellet-Plamondon, C.M. Electrical and thermal
458 conductivity of ethylene vinyl acetate composite with graphene and carbon black filler. *Polym. Test.* 2018,
459 72, 24-31.

- 460 67. Azizi, S.; David, E.; Fréchet, M.F.; Nguyen-Tri, P.; Ouellet-Plamondon, C.M. Electrical and thermal
461 phenomena in low-density polyethylene/carbon black composites near the percolation threshold. *J. Appl.*
462 *Polym. Sci.* 2018, 47043.
- 463 68. Boukehili, H.; Nguyen-Tri, P. Helium gas barrier and water absorption behavior of bamboo fiber reinforced
464 recycled polypropylene. *J. Reinf. Plast. Compos.* 2012, 31, 1638–1651. [Google Scholar]
- 465 69. Nguyen Tri, P.; Gilbert, V. Non-isothermal Crystallization Kinetics of Short Bamboo Fiber-reinforced
466 Recycled Polypropylene Composites. *J. Reinf. Plast. Compos.* 2010, 29, 2576–2591. [Google Scholar]
- 467 70. Nguyen Tri, P.; Sollogoub, C.; Guinault, A. Relationship between fiber chemical treatment and properties
468 of recycled pp/bamboo fiber composites. *J. Reinf. Plast. Compos.* 2010, 29, 3244–3256. [Google Scholar]
- 469 71. Tri, P.N.; Rtimi, S.; Nguyen, T.A.; Vu, M.T. Physics, Electrochemistry, Photochemistry, and
470 Photoelectrochemistry of Hybrid Nanoparticles. In *Noble Metal-Metal Oxide Hybrid Nanoparticles*;
471 Woodhead Publishing: Sawston, UK, 2019; pp. 95–123.
- 472 72. Nguyen Tri, P.; Ouellet-Plamondon, C.; Rtimi, S.; Assadi, A.A.; Nguyen, T.A. Methods for Synthesis of
473 Hybrid Nanoparticles. In *Noble Metal-Metal Oxide Hybrid Nanoparticles*; Woodhead Publishing:
474 Sawston, UK, 2019; pp. 51–63.
- 475 73. Nguyen, T.V.; Nguyen Tri, P.; Nguyen, T.D.; El Aidani, R.; Trinh, V.T.; Decker, C. Accelerated degradation
476 of water borne acrylic nanocomposites used in outdoor protective coatings. *Polym. Degrad. Stab.* 2016,
477 128, 65–76.
- 478 74. Nguyen Tri, P.; Prud'homme, R.E. Crystallization and Segregation Behavior at the Submicrometer Scale of
479 PCL/PEG Blends. *Macromolecules* 2018, 51, 7266–7273. [Google Scholar] [CrossRef]
- 480 75. Nguyen, T.P. Nanoscale analysis of the photodegradation of Polyester fibers by AFM-IR. *J. Photochem.*
481 *Photobiol. A Chem.* 2018, 371, 196–204.
- 482 76. Tri, P.N.; Prud'homme, R.E. Nanoscale Lamellar Assembly and Segregation Mechanism of Poly(3-
483 hydroxybutyrate)/Poly(ethylene glycol) Blends. *Macromolecules* 2018, 51, 181–188.
- 484 77. El Aidani, R.; Nguyen-Tri, P.; Malajati, Y.; Lara, J.; Vu-Khanh, T. Photochemical aging of an e-
485 PTFE/NOMEX® membrane used in firefighter protective clothing. *Polym. Degrad. Stabi.* 2013, 98, 1300–
486 1310.
- 487 78. Zeb, G.; Tri, P.N.; Palacin, S.; Le, X.T. Pulse potential deposition of thick polyvinylpyridine-like film on the
488 surface of titanium nitride. *RSC Adv.* 2016, 6, 80825–80829.
- 489 79. Nguyen, T.V.; Le, X.H.; Dao, P.H.; Decker, C.; Nguyen-Tri, P. Stability of acrylic polyurethane coatings
490 under accelerated aging tests and natural outdoor exposure: The critical role of the used photo-stabilizers.
491 *Prog. Org. Coat.* 2018, 124, 137–146.
- 492